

ChemComm

Chemical Communications

www.rsc.org/chemcomm

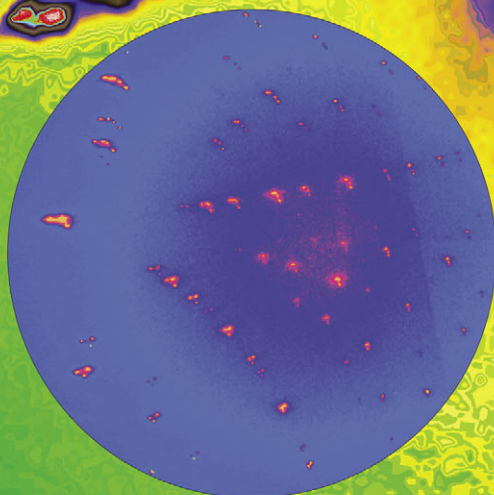
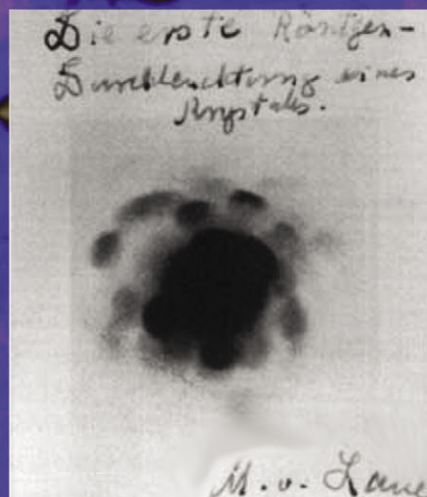
Volume 48 | Number 16 | 21 February 2012 | Pages 2157–2256

100 years of ...

2012

1912

... Laue diffraction



ISSN 1359-7345

RSC Publishing

COMMUNICATION

Oliver Oeckler *et al.*

From metastable to stable modifications—*in situ* Laue diffraction investigation of diffusion processes during the phase transitions of $(\text{GeTe})_n\text{Sb}_2\text{Te}_3$ ($6 < n < 15$) crystals



1359-7345(2012)48:16;1-B

Cite this: *Chem. Commun.*, 2012, **48**, 2192–2194

www.rsc.org/chemcomm

COMMUNICATION

From metastable to stable modifications—*in situ* Laue diffraction investigation of diffusion processes during the phase transitions of $(\text{GeTe})_n\text{Sb}_2\text{Te}_3$ ($6 < n < 15$) crystals†Matthias N. Schneider,^a Xavier Biquard,^b Christian Stiewe,^c Thorsten Schröder,^a Philipp Urban^{ad} and Oliver Oeckler^{*ad}

Received 19th September 2011, Accepted 15th November 2011

DOI: 10.1039/c1cc15808b

Temperature dependent phase transitions of compounds $(\text{GeTe})_n\text{Sb}_2\text{Te}_3$ ($n = 6, 12, 15$) have been investigated by *in situ* microfocus Laue diffraction. Diffusion processes involving cation defect ordering at ~ 300 °C lead to different nanostructures which are correlated to changes of the thermoelectric characteristics.

Thermodynamically stable phases of GeTe-rich compounds $(\text{GeTe})_n\text{Sb}_2\text{Te}_3$ ($n > 3$) exhibit rocksalt-type high-temperature (HT) phases but crystallize in trigonal long-periodically ordered layered structures at room temperature (RT) (*cf.* Fig. 1).^{1,2} The latter exhibit no cation vacancies but are composed of distorted rocksalt-type slabs with $2n + 5$ alternating cation and anion layers which are interconnected *via* van der Waals gaps between Te atom layers terminating the slabs. In contrast, the HT phases contain $1/(n + 3)$ cation defects per anion randomly distributed.³ Both modifications are related by a phase transition which involves diffusion—formally of cation defects which form layers at low temperature—and by the alteration of the cubic stacking sequence of Te atom layers to yield van der Waals gaps. Metastable modifications obtained by quenching the HT phases represent an “intermediate state” of this transition. They exhibit domains with a trigonally distorted rocksalt-type average structure which are eight-fold twinned according to the group-subgroup relationship $Fm\bar{3}m \rightarrow R\bar{3}m \rightarrow R3m$.⁴ The deviation from the cubic metrics increases with increasing n .¹ Diffraction patterns of quenched samples exhibit pseudo-cubic symmetry due to the incoherent superposition of intensities from individual domains. Short-range defect ordering produces nanostructures characterized by intersecting vacancy layers perpendicular to the pseudo-cubic

$\langle 111 \rangle$ directions (*cf.* Fig. 1), as indicated by diffuse scattering (DS) and electron microscopy.^{3,4}

Metastable modifications are important in write-erase cycles of modern data storage media such as Blu-Ray Discs or non-volatile PC-RAM. Furthermore, they are an intriguing class of thermoelectrics with figures of merit ZT of up to 1.3.^{4,5} Both these applications strongly depend on physical properties related to the real structure of the materials.^{6,7} Therefore, it is of great interest to study temperature-dependent diffusion processes associated with the phase transitions of $(\text{GeTe})_n\text{Sb}_2\text{Te}_3$ compounds.

Micro-focus white-beam (Laue) diffraction using synchrotron radiation is an intriguing method for such investigations. Micro-focusing partially excludes space-averaging effects typical for conventional X-ray diffraction experiments, whereas due to the polychromatic beam large areas of reciprocal space are recorded in a single frame. Laue diffraction

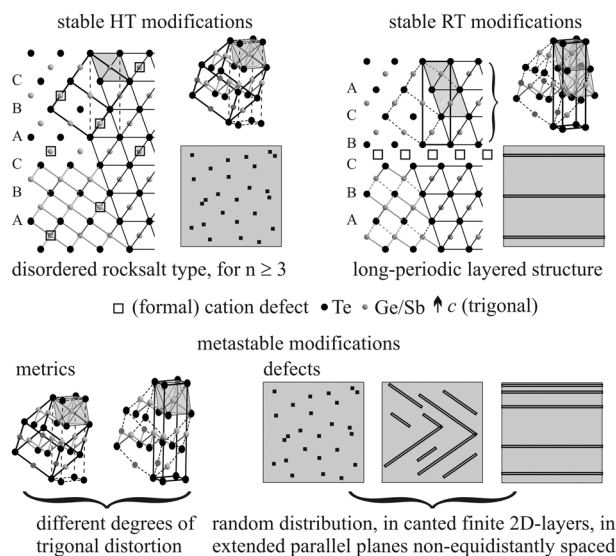


Fig. 1 Structures of different modifications of $(\text{GeTe})_n\text{Sb}_2\text{Te}_3$ phases with schematic representations of different cation defect distributions: sections of stable phases (top, along $[010]$, trigonal setting), perspective views indicate the rocksalt-type building units (cubic and trigonal cells are outlined); bottom left: average structure of metastable phases with more or less pronounced distortion.

^a Department of Chemistry, LMU Munich, Butenandtstrasse 5-13 (D), 81377 Munich, Germany. E-mail: oliver.oeckler@gmx.de;

Fax: +49 (0)89-2180-77440; Tel: +49 (0)89-2180-77421

^b CEA-Grenoble, DSM/INAC, 17 avenue des Martyrs, 38054 Grenoble Cedex 9, France

^c German Aerospace Centre, Linder Höhe, 51147 Cologne, Germany

^d IMKM, University of Leipzig, Scharnhorststr. 20, 04275 Leipzig, Germany

† Electronic supplementary information (ESI) available: Experimental details, Fig. S1–S4, additional Laue diffraction patterns at various temperatures of the three samples investigated with selected predicted Bragg positions according to indexing. See DOI: 10.1039/c1cc15808b

patterns of various GeTe-rich $(\text{GeTe})_n\text{Sb}_2\text{Te}_3$ crystals grown by chemical transport reactions were collected at BM32 (ESRF, Grenoble) using a micro-beam (focus $< 1 \times 1 \mu\text{m}^2$) in a temperature range from RT to $\sim 600^\circ\text{C}$ (accuracy $\pm 15^\circ\text{C}$). Details of the sample preparation and the experimental setup can be found in the ESI.†

Laue diffraction patterns of a crystal of $\text{Ge}_{0.65(3)}\text{Sb}_{0.22(1)}\text{Te} = (\text{GeTe})_6\text{Sb}_2\text{Te}_3$, which was grown in the stability range of the cubic HT phase and subsequently quenched (*cf.* Fig. 2), show asymmetrically broadened reflections interconnected by diffuse streaks. The variation of both the asymmetric broadening as well as the DS in patterns collected at different positions on the sample corresponds to the presence of individual twin domains which are at least as large as the area irradiated by the micro-beam. The broadening of the Bragg reflections is related to the varying metric distortion of individual domains along one of the pseudocubic $\langle 111 \rangle$ directions. It is further enhanced due to short-range order. The orientation of the diffuse streaks between the Bragg positions continues the asymmetric broadening and indicates the presence of extended planar defects which are parallel but not equidistant. Upon heating ($10^\circ\text{C min}^{-1}$; *cf.* Fig. S1a†), between 250 and 300°C the diffuse streaks gradually transform into a series of rather sharp reflections characteristic of a long-periodic layered structure (*cf.* Fig. 2, bottom left). The reflections observed in zones with variable l roughly match with a 51R-type structure.¹ This is in accordance with the cation/anion ratio of $(\text{GeTe})_6\text{Sb}_2\text{Te}_3$ which determines the thickness of the rocksalt-type slabs.² However, such a structure prediction on the basis of simple rules is limited by non-stoichiometry⁸ so that details of the structure cannot unequivocally be determined. At $\sim 500^\circ\text{C}$, the characteristic reflections of the layered structure become weak and at 550°C the cubic HT modification is formed. The diffraction pattern above this temperature (Fig. 2, bottom right) can be indexed assuming a cF lattice with $a = 6.00 \text{ \AA}$ (*cf.* Fig. S2a†) in accordance with lattice parameters reported for such HT modifications.^{1,3} The absence of structured DS confirms the random arrangement of the cation defects.

A similar experiment with a metastable $\text{Ge}_{0.83(4)}\text{Sb}_{0.14(1)}\text{Te} = (\text{GeTe})_{12}\text{Sb}_2\text{Te}_3$ crystal (*cf.* Fig. S1b and S3†) shows very broad reflections at RT whose broadening does not exhibit a preferred direction, and there are no distinct diffuse streaks. These data indicate the absence of domains with parallel planar defects larger than the beam size; they rather correspond to twinning on the nanoscale. Upon heating, the DS becomes more structured at 350°C and gradually develops into streaks. At 400°C , the Bragg reflections are sharp and correspond to an hR lattice with $a/c = 0.404$ ($a = 4.25 \text{ \AA}$, $c = 10.52 \text{ \AA}$). They are interconnected by diffuse streaks along c^* corresponding to parallel but not equidistant defect planes. When the temperature is further increased ($\sim 10^\circ\text{C min}^{-1}$), the streaks do not transform into rows of sharp reflections. Instead, from 450°C on their intensity gradually decreases. The absence of structured DS at 500°C indicates a random defect distribution; the Bragg reflections can be indexed based on a rocksalt-type cell with $a = 6.00 \text{ \AA}$ (*cf.* Fig. S2b†). Thermal cycling experiments reveal that this HT modification can be undercooled to about 30°C before a disordered layered structure is reformed. Diffuse streaks become clearly visible between $430\text{--}370^\circ\text{C}$. Upon reheating,

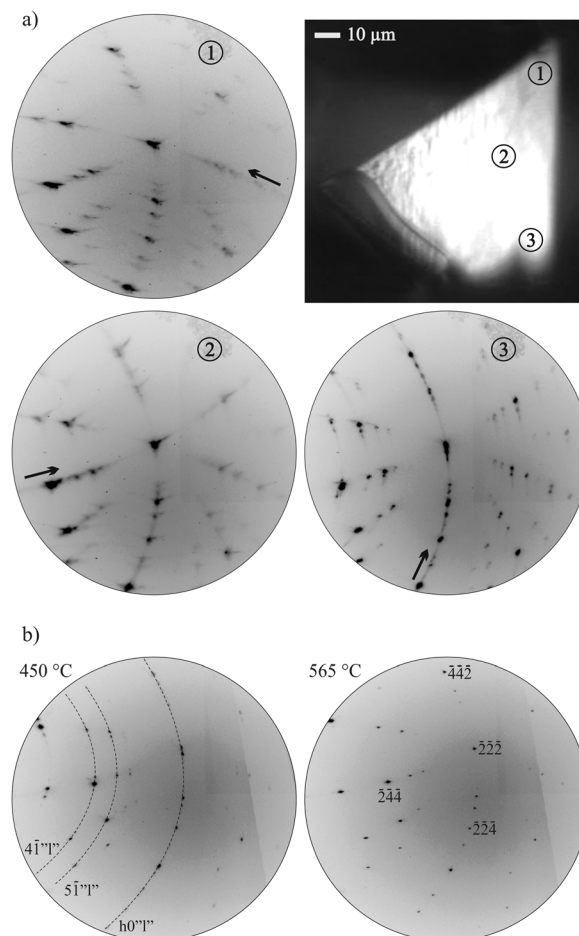


Fig. 2 (a) Optical microscopy image of the $(\text{GeTe})_6\text{Sb}_2\text{Te}_3$ crystal (top right) and RT Laue frames collected from the positions indicated by the numbers (black arrows indicate the main orientation of diffuse streaks); (b) patterns collected from position 3 (slightly different section of the pattern) at 450°C (selected rays of the $h\bar{1}l$ plane and the $h0l$ zone are indicated) and at 565°C (with selected indices).

the intensity of these streaks decreases from 500°C on; however, the rocksalt-type phase without DS forms at slightly higher temperature compared to the initial heating.†

Although both $(\text{GeTe})_6\text{Sb}_2\text{Te}_3$ and $(\text{GeTe})_{12}\text{Sb}_2\text{Te}_3$ exhibit a similar HT modification, the real structure of quenched crystals is significantly different. As a consequence of the higher vacancy concentration, short-range defect ordering is more pronounced in $(\text{GeTe})_6\text{Sb}_2\text{Te}_3$ and yields extended, parallel defect planes, whereas in $(\text{GeTe})_{12}\text{Sb}_2\text{Te}_3$, the diffraction data indicate a nanostructure with finite intersecting defect layers.^{4,7} The diffusion pathways required to form a long-periodic structure are shorter for $(\text{GeTe})_6\text{Sb}_2\text{Te}_3$. Therefore, the ordered structure appears within a few seconds when diffusion sets in at 300°C . Although diffusion is activated in a similar temperature range in $(\text{GeTe})_{12}\text{Sb}_2\text{Te}_3$, extended defect layers are not formed until the cubic high-temperature phase appears. In this case, the formation of a long-periodically ordered structure requires prolonged annealing times.^{1,3,4}

Laue diffraction patterns of quenched $\text{Ge}_{0.84(1)}\text{Sb}_{0.12(1)}\text{Te} = (\text{GeTe})_{15}\text{Sb}_2\text{Te}_3$ crystals (Fig. 3) do not show strongly broadened Bragg reflections at RT, in contrast to samples with lower

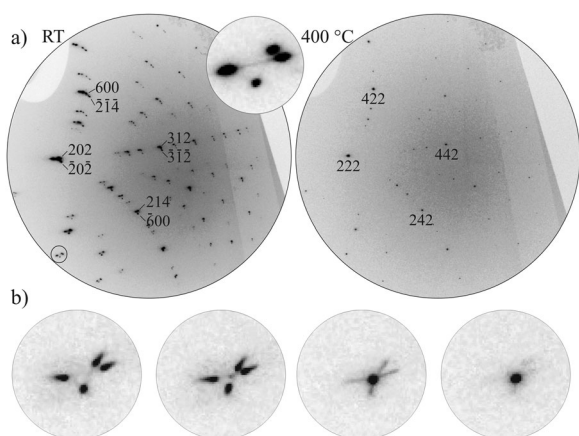


Fig. 3 (a) Laue diffraction patterns of $(\text{GeTe})_{15}\text{Sb}_2\text{Te}_3$ collected at RT and at 400 °C, the inset shows an enlarged group of reflections from different domains (exemplary indices are given); (b) changing intensity distribution of the reflection group indicated in (a) between 330 and 340 °C (left to right) during heating.

GeTe content. Groups of reflections result from the superposition of the intensities from individual domains with unit cells clearly deviating from pseudo-cubic metrics. Reflections belonging to individual domains can be indexed based on an hR cell with $a = 4.22 \text{ \AA}$ and $c = 10.57 \text{ \AA}$ (cf. Fig. S4†). The ratio $a/c = 0.399$ lies between that of $\alpha\text{-GeTe}$ ($a/c = 0.389$)⁹ and that of a cubic cell in hR setting ($a/c = 0.408$). Whereas no DS is observed between groups of reflections, there are weak diffuse streaks that interconnect the reflections of one group. These are due to domain-wall scattering (cf. Fig. 3 and Fig. S4†). Upon heating above 330 °C, additional Bragg reflections of the rocksalt-type HT phase appear in between the reflections of each group and gain intensity as the rhombohedral distortion of the individual domains decreases. At 400 °C only reflections which can be indexed with a cF cell with $a = 6.00 \text{ \AA}$ are observed (cf. Fig. 3 and S2c†). In contrast to samples with lower GeTe contents, $(\text{GeTe})_{15}\text{Sb}_2\text{Te}_3$ shows no pronounced nanostructures. At all temperatures, there was no DS indicative of extended planar faults. Intrinsic cation defects can be assumed to concentrate at domain boundaries. However, slightly below the transition temperature to the cubic HT modification, trigonal and cubic domains coexist. Although the $(\text{GeTe})_{15}\text{Sb}_2\text{Te}_3$ crystal can be viewed as a multiply twinned Sb_2Te_3 -doped variant of GeTe, the phase transition is different from the displacive rhombohedral to cubic transition of GeTe at $\sim 432 \text{ }^\circ\text{C}$ ^{9,10} as it requires diffusion of defects from domains boundaries to form the disordered rocksalt type. Upon cooling the crystal below 330 °C, the sharp reflections of the HT modification significantly broaden and the patterns resemble those observed for $(\text{GeTe})_{12}\text{Sb}_2\text{Te}_3$ at RT (cf. Fig. S5†). This indicates that a nano-domain transformation twin is formed, whereas before heating a growth twin was present.

Metastable Ge–Sb–Te phases are p-type semiconductors with rather low thermal conductivities, κ , rendering them promising candidates for thermoelectric materials. Fig. 4 shows the temperature dependence of κ of quenched samples $(\text{GeTe})_n\text{Sb}_2\text{Te}_3$ ($n = 7, 12, 19$) as well as the Seebeck coefficient and the electrical conductivity of $(\text{GeTe})_{12}\text{Sb}_2\text{Te}_3$ (for experimental details refer to ESI†).§ The thermal conductivity curves are discontinuous:

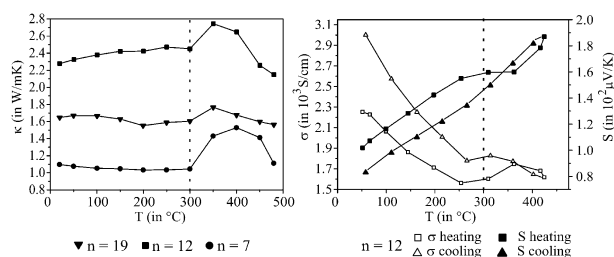


Fig. 4 Thermal conductivities of quenched $(\text{GeTe})_n\text{Sb}_2\text{Te}_3$ ($n = 7, 12, 19$) (left); and temperature dependency of the Seebeck coefficients and the electrical conductivity σ of metastable $(\text{GeTe})_{12}\text{Sb}_2\text{Te}_3$ (right).

above 300 °C, κ increases by $\sim 0.2 \text{ W m}^{-1} \text{ K}^{-1}$ and decreases again at higher temperature. At similar temperatures, the Seebeck coefficient and σ of $(\text{GeTe})_{12}\text{Sb}_2\text{Te}_3$ change discontinuously and show a hysteretic behavior.

Several conclusions can be drawn from our experiments: the high-temperature phase transitions of $(\text{GeTe})_n\text{Sb}_2\text{Te}_3$ ($n > 3$) involve the rearrangement of cation defects and therefore are predominantly order–disorder transitions rather than displacive phase transitions such as that of GeTe. For all samples, diffusion processes are activated at $\sim 300 \text{ }^\circ\text{C}$. This is mirrored in the thermoelectric characteristics. The diffusion processes influence the thermal conductivities and also alter the electronic structure. The hysteresis of the properties concurs with the limited mobility of defects. Our investigation clearly demonstrates that investigations of the average structure, e.g. by powder diffraction, are not sufficient to understand the relevant temperature dependent structure–property relationships of these materials because the diffusion processes and thus the changes of the real structure are predominantly reflected as diffuse scattering.

We thank M. Szebenyi for supporting the Daresbury Software Suite. We gratefully acknowledge funding by the Deutsche Forschungsgemeinschaft (grant OE530/1-2) and thank T. Miller and C. Minke for technical support. We are indebted to Prof. Dr. W. Schnick for his generous support of this work.

Notes and references

† The HT modification of $(\text{GeTe})_6\text{Sb}_2\text{Te}_3$ can also be undercooled to about 30 °C, however, no thermal cycling experiments were performed.
§ The dependency of the thermoelectric properties on the composition is discussed elsewhere.⁷

- 1 D. T. Matsunaga, H. Morita, R. Kojima, N. Yamada, K. Kifune, Y. Kubota, Y. Tabata, J.-J. Kim, M. Kobata, E. Ikenaga and K. Kobayashi, *J. Appl. Phys.*, 2008, **103**, 093511.
- 2 O. G. Karpinsky, L. E. Shelimova, M. A. Kretova and J.-P. Fleurial, *J. Alloys Compd.*, 1998, **268**, 112.
- 3 M. N. Schneider, T. Rosenthal, C. Stiewe and O. Oeckler, *Z. Kristallogr.*, 2010, **225**, 463.
- 4 M. N. Schneider, P. Urban, A. Leineweber, M. Döblinger and O. Oeckler, *Phys. Rev. B*, 2010, **81**, 184102.
- 5 D. Lencer, M. Salina and M. Wuttig, *Adv. Mater.*, 2011, **23**, 2030.
- 6 T. Siegrist, P. Jost, H. Volker, M. Woda, P. Merkelbach, C. Schlockermann and M. Wuttig, *Nat. Mater.*, 2011, **10**, 202.
- 7 T. Rosenthal, M. N. Schneider, C. Stiewe, M. Döblinger and O. Oeckler, *Chem. Mater.*, 2011, **23**, 4349.
- 8 M. N. Schneider and O. Oeckler, *Z. Anorg. Allg. Chem.*, 2008, **634**, 2557.
- 9 T. Chattopadhyay, J. X. Boucherle and H. G. von Schnering, *J. Phys. C: Solid State Phys.*, 1987, **20**, 1431.
- 10 A. V. Kolobov, M. Krbal, P. Fons, J. Tominaga and T. Uruga, *Nat. Chem.*, 2011, **3**, 311.